Journal of
Plankton Research

academic.oup.com/plankt

J. Plankton Res. (2022) 44(3): 443–453. First published online April 23, 2022 https://doi.org/10.1093/plankt/fbac019

ORIGINAL ARTICLE

Comparison of population structure, vertical distribution and growth of sympatric, carnivorous, mesopelagic copepods, *Paraeuchaeta glacialis* and *Heterorhabdus norvegicus*, in the western Arctic Ocean

ATSUSHI YAMAGUCHI[1,2,*], CARIN J. ASHJIAN[3] AND ROBERT G. CAMPBELL[4]

[1]GRADUATE SCHOOL OF FISHERIES SCIENCES, HOKKAIDO UNIVERSITY, 3-1-1 MINATO-CHO, HAKODATE, HOKKAIDO 041-8611, JAPAN, [2]ARCTIC RESEARCH CENTER, HOKKAIDO UNIVERSITY, KITA-21 NISHI-11 KITA-KU, SAPPORO, HOKKAIDO 001-0021, JAPAN, [3]BIOLOGY DEPARTMENT, WOODS HOLE OCEANOGRAPHIC INSTITUTION, 266 WOODS HOLE RD., WOODS HOLE, MA 02543, USA AND [4]GRADUATE SCHOOL OF OCEANOGRAPHY, UNIVERSITY OF RHODE ISLAND, NARRAGANSETT, RI, 02882, USA

*CORRESPONDING AUTHOR: a-yama@fish.hokudai.ac.jp

Received March 7, 2021; editorial decision March 23, 2022; accepted March 23, 2022

Corresponding editor: Marja Koski

In the Arctic Ocean, the life cycles of interzonal omnivorous copepods have been studied, whereas little information is available on the life cycles of mesopelagic carnivorous species. Here, the life cycles of two mesopelagic carnivorous copepods (*Paraeuchaeta glacialis* and *Heterorhabdus norvegicus*) are described from vertically stratified samples collected at an annual ice-station (SHEBA) in the western Arctic Ocean during 1996–1997. Reproduction estimated to occur between January and March for both species. Vertical distributions and population growth varied between the species. Early copepodite stages and adult males of *P. glacialis* were distributed in deeper layers, whereas late copepodite stages and adult females were observed in shallower layers. The skewed sex ratio towards females was observed for adults, which may be related to the cease feeding and short longevity for adult males. In contrast, all the *H. norvegicus* life stages were distributed in the mesopelagic layer. Clear peaks of the young stages and their sequence suggest that *H. norvegicus* may complete its life cycle within 1 year. A specialized feeding mode (incorporating a venomous injection spine and large

available online at academic.oup.com/plankt

beak) could be a key trait facilitating the achievement of rapid growth in *H. norvegicus* in the food-limited mesopelagic layer.

KEYWORDS: Arctic Ocean; Carnivorous copepods; Growth rate; Life cycle

INTRODUCTION

In the Arctic Ocean, seasonal changes in daylight length and ice cover influence the population and activity dynamics of organisms (Steele and Dickinson, 2016 and references therein). In response to the considerable seasonal and environmental fluctuations, primary productivity exhibits clear seasonality (Bélanger *et al*., 2013; Ji *et al*., 2013). Mesozooplankton, particularly copepods, are the major secondary producers in the Arctic Ocean (Kosobokova, 1982; Kosobokova and Hirche, 2000). Most studies on the life cycles of Arctic copepods have focused on the large interzonal omnivorous copepods: *Calanus hyperboreus, Calanus glacialis* and *Metridia longa* and have shown that the life events of these species, such as reproduction and development, are well synchronized with phytoplankton bloom (Conover, 1988; Ashjian *et al*., 2003; Søreide *et al*., 2010). In contrast, information on the life cycles of mesopelagic copepod species with other feeding modes (carnivores or detritivores) is limited.

Two mesopelagic carnivorous copepods, *Paraeuchaeta glacialis* and *Heterorhabdus norvegicus*, are abundant throughout the Arctic Ocean (Kosobokova and Hirche, 2000; Kosobokova and Hopcroft, 2010; Kosobokova *et al*., 2011). In the Arctic Ocean, *P. glacialis* accounts for 1–2% of mesozooplankton and 1–8% of the copepod biomass (Kosobokova, 1982; Kosobokova and Hirche, 2000; Kosobokova and Hopcroft, 2010). In addition, *P. glacialis* accounts for 3% of the food-item biomass of the Arctic cod (*Boreogadus saida*) and is the third most important copepod prey species, after *C. hyperboreus* and *C. glacialis* (Majewski *et al*., 2016). The year-round presence of egg-carrying females of *P. glacialis* has been reported (Johnson, 1963), in addition to a sex ratio skewed towards females (Dvoretsky and Dvoretsky, 2015). Based on the results of vertically stratified sampling activities, *P. glacialis* males in the early copepodite and adult stages are abundant at depths of 500 m or greater, and the copepodites ascend to shallower depths during development from copepodite stages 1–5 (C1–C5) (Yamaguchi *et al*., 2019). Such ontogenetic migration behavior combined with increment in weight at each stage being greater than that for the shallow-depth inhabiting stages suggests that the upward ontogenetic migration is associated with their raptorial feeding and food (prey) availability (Yamaguchi *et al*., 2019). Although such information would be valuable for understanding deep-sea biology, seasonal changes in the population structure and life cycle of *P. glacialis* in the Arctic Ocean are relatively unknown.

H. norvegicus is spread over the entire geographical range of the Arctic Ocean (Kosobokova, 1982; Kosobokova and Hirche, 2000; Kosobokova and Hopcroft, 2010; Smoot and Hopcroft, 2017). In contrast to *P. glacialis*, the adult sex ratio of *H. norvegicus* is reportedly skewed towards males (Tokuhiro *et al*., 2019). *Heterorhabdus* species have a specialized mouthpart morphology and feeding modes. They are capable of injecting venom via a mandibular tooth and labral glands (Nishida and Ohtsuka, 1996) and use a large beak in the labrum–paragnath complex as a feeding apparatus (Lewis, 2014). Furthermore, *H. norvegicus* has the smallest eggs amongst the 14 species whose reproductive behavior and egg production have been studied in the Arctic Ocean (Kosobokova *et al*., 2007). The specialized *H. norvegicus* feeding mode and egg size characteristics are distinct from *P. glacialis*. However, a comparison of the ecology of these two species is not researched.

In this study, we quantified populations and measured the weights of each stage of *P. glacialis* and *H. norvegicus* from vertically stratified samples collected at an ice-station (SHEBA, Ashjian *et al*., 2003) in the western Arctic Ocean from October 1996 to September 1997. We aimed to evaluate and compare the ecological characteristics (population structure, vertical distribution and growth) of the two sympatric mesopelagic carnivorous copepods in the Arctic Ocean. Through these data, we calculate the growth rates of each species and discuss the mechanism of the sympatric carnivorous copepods to maintain their population in the mesopelagic layer of the Arctic Ocean.

METHODS

Zooplankton samples were collected during a Surface Heat Budget of the Arctic Ocean (SHEBA) expedition (e.g. Ashjian *et al*., 2003), which drifted through the Canada Basin to the Mendeleev Plain between October 1997 and September 1998 (Supplemental material 1 [Fig. S1]). Stratified vertical hauls (normally 0–50 m, 50–100 m, 100–200 m, 200–1500 m and 1500–2800 m, depending on bottom depth) were made above the seafloor at 10–14-day intervals (total 30

sampling dates) using a 1-m^2 mouth area opening–closing net equipped with 150-μm mesh (Ashjian *et al.*, 2003). The samples were preserved in 4% buffered formalin-seawater. Vertical temperature profiles were collected using conductivity-temperature-depth (CTD) sensors.

We sorted and counted all copepodite stages of *P. glacialis* and *H. norvegicus* in each sample. Morphological differentiation of females and males was possible for stages C4 to adults in *P. glacialis*. The females lack swimming leg 5, whereas males have leg 5 in C4–C6 (Campbell, 1934). Since sex separation was possible for C4–C6 *P. glacialis*, their stage composition within each sex was compared and tested by one-way analysis of variance (ANOVA) and post hoc Tukey–Kramer test. In *H. norvegicus*, separation of the sexes was only possible at stage C6 (See Supplemental material 2 [Fig. S2] [*P. glacialis*] and 3 [Fig. S3] [*H. norvegicus*] for details of each copepodite stage). All *P. glacialis* copepodite stages were observed in the samples. In the case of *H. norvegicus*, only stages C3 and older occurred in the samples. Based on the prosome widths (PWs) of the observed stages and the diagonal lengths of the net mesh used (212 μm), we assume the above-mentioned stages were quantitatively collected (PW of *P. glacialis* C1 was 335 ± 23 μm [mean $\pm$ 1sd, $n = 10$], PW of *H. norvegicus* C3 was 250 ± 29 μm [$n = 4$]). Specimens with spermatophores attached in the case of adult females (C6F) for both species (Supplemental material 2 [Fig. S2] and 3 [Fig. S3]) were counted separately. In *P. glacialis* (C6F), egg-carrying individuals were also observed and counted separately. For egg sacs, the substantial numbers with detached were observed in the samples. However, since we did not quantify the detached egg sacs in the samples species identification via egg sacs was uncertain.

Sympatric sibling species, *Paraeuchaeta barbata* and *Paraheterorhabdus compactus*, occurred in the samples for each species. Because the sibling species had relatively fat body shapes, their PWs were larger than those of *P. glacialis* and *H. norvegicus* at the same stages, especially in C1–C3. In addition, their occurrence at greater depths in the water column confirmed their species identity.

Seafloor depth was in the 352–3850-m range over the year-long drift (Ashjian *et al.*, 2003). The number of depth intervals sampled on each date changed from two to eight (Supplemental material 4 [Table S1] and 5 [Table S2]) partially because of the variation in seafloor depth. As *P. glacialis* and *H. norvegicus* are primarily found at depths greater than 250 m (see below, Fig. 4a), samples collected at depths shallower than 400 m were not considered, reducing the number of available sampling dates to 20 from an original 30. The successive dates obtained were separated by at most 1 month, permitting analysis of seasonal abundance and population structure (Supplemental material 4 [Table S1] and 5 [Table S2]).

The core depth distribution ($D_{50\%}$) was calculated based on abundance (ind. m^{-2}) in each sampling layer (Yamaguchi *et al.*, 2020):

$$D_{50\%} = d_1 + (d_2 - d_1) \times \frac{50 - p_1}{p_2}$$

where d_1 is the depth (m) of the upper depth of the 50% individual occurrence layer, d_2 is the maximum depth (m) of the 50% individual occurrence layer, p_1 is the cumulative individual percentage (%) that occurred at depths shallower than the 50% individual occurrence layer and p_2 is the individual percentage (%) at the 50% individual occurrence layer. The means and standard deviations of the $D_{50\%}$ of each copepodite stage were calculated during the polar night (mid-November–early February) and the midnight sun (late April–August). The differences were tested using the Mann–Whitney U-test. Dates with maximum sampling depths shallower than 900 m or collected during transition periods between the midnight sun and polar night were omitted from the descriptions of vertical distributions, retaining three dates during the midnight sun and six dates during the polar night (Supplemental material 4 [Table S1] and 5 [Table S2]). Ontogenetic changes in vertical distribution during the midnight sun and polar night were tested using one-way ANOVA based on the $D_{50\%}$ of each copepodite stage.

Prosome length (PL), wet weight (WW), dry weight (DW) and ash-free dry weight (AFDW) were measured for each stage using formalin-preserved samples. Copepodite stages were selected and photographed using a stereomicroscope. PL was measured in images at a 10-μm precision using ImageJ (https://imagej.nih.gov/ij/). WW was determined for pooled specimens (2–21 individuals of each stage) that had been rinsed briefly in distilled water, blotted dry on a filter paper and weighed in a preweighed combusted aluminum pan. *P. glacialis* weights were also measured for individual egg sacs and nauplius. Samples were dried in an oven at 60°C for 5 h and then reweighed to determine DW. Ash content was determined by reweighing the same samples after combusting them at 480°C for 5 h. AFDW was then determined based on the difference. All weights were determined to a precision of 1 μg using a CAHN (C-33) microbalance. To determine the stages when PL and weight growth occurred, the proportions of growth (PG, %) that occurred at C_{n-1}/C_n for PL, WW, DW and AFDW were determined for females and males, treating the values of adults as 100% (Yamaguchi *et al.*, 2020):

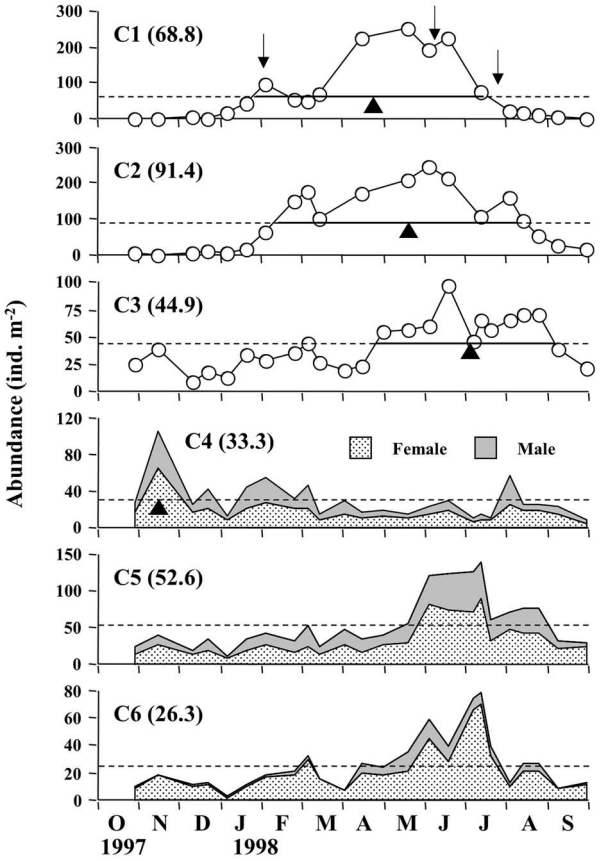

Fig. 1. *Paraeuchaeta glacialis*. Seasonal abundance of copepodite stages in the western Arctic Ocean. Females and males were distinguishable at C4–C6. Values in the parentheses and horizontal broken lines indicate the annual mean abundance of each stage. Three arrows in the top panel indicate timings of water mass changes (cf. Ashjian *et al*. 2003). For calculation of growth rate, the abundant periods of C1–C3 (greater than means) were marked with solid horizontal lines and indicated their middle dates by solid triangles. For the consecutive C4, their peak abundance date marked with solid triangle was also used for the growth rate calculation.

PG = 100 × (value of C_n–value of C_{n-1})/value of adult (C6).

Based on the individual DW and abundant date of each copepodite stage, the weight-specific growth rate (g, day^{-1}) was calculated for each species (Hirst *et al*., 2003):

$$g = (\ln W_t - \ln W_0)/t.$$

where W_0 is DW at time zero, W_t is DW at time t and t is the time in days. The growth rate calculation was made for C1–C4 of *P. glacialis* and for C4–C6 of *H. norvegicus*, of which stages that consecutive traces of the growth of the cohorts were possible. For the reached dates of each copepodite stage, the middle dates of the abundant period (C1–C3 of *P. glacialis* and C6 of *H. norvegicus*) or the peak of each copepodite stage (C4 of *P. glacialis* and C4–C5 of *H. norvegicus*) were applied. The applied dates were marked by the symbols of the solid triangles in Figs. 1 and 3. The exact dates of applied dates for each copepodite stage are shown in Supplemental material 4 (Table S1) and 5 (Table S2).

Table I: Sex ratio (% of females in total adult) of Paraeuchaeta glacialis and Heterorhabdus norvegicus based on year-round (1997–1998) observations at ice station SHEBA in the western Arctic Ocean

Species Stage	Annual mean
P. glacialis	
C4	59.4 ± 3.9
C5	59.3 ± 3.7
C6	81.9 ± 6.1
H. norvegicus	
C6	44.1 ± 11.3

Values are annual mean ± standard error (SE). Note that sex separation was possible for C4–C6 in *P. glacialis* but only for C6 in *H. norvegicus*.

RESULTS

Population structure

P. glacialis

Clear seasonal abundance patterns were observed for each stage (Fig. 1). C1 was abundant from February to July (peaked from April to June), C2 from February to August, C3 from May to September, C4 from August to February and both C5 and C6 were widespread from May to August. The sex ratio was skewed slightly towards females in C4 and C5 (females comprised 59.3–59.4% in the whole population) (Table I) and clearly towards females in C6 (females comprised 81.9%). For both sexes, stage composition in C4–C6 was dominated by C5 ($P < 0.0001$; one-way ANOVA, $P < 0.05$; Tukey–Kramer) (Fig. 2). The abundant seasons of each stage were similar for both sexes. C4 was abundant during October to February, C5 from February to September and C6 from February to July (Fig. 2). Adult females (C6F) with spermatophores attached were abundant from July to August and comprised up to 22% of the total C6F on 11 July. Egg-carrying C6F was abundant from March to July and comprised up to 37% of the females on 14 April.

H. norvegicus

Clear seasonal abundance trends were also detected for each copepodite stage of *H. norvegicus* (Fig. 3). Stage C3 was generally absent or in low abundance, excluding a brief peak in August; C4 was abundant from December to March; C5 from January to April and C6 from January

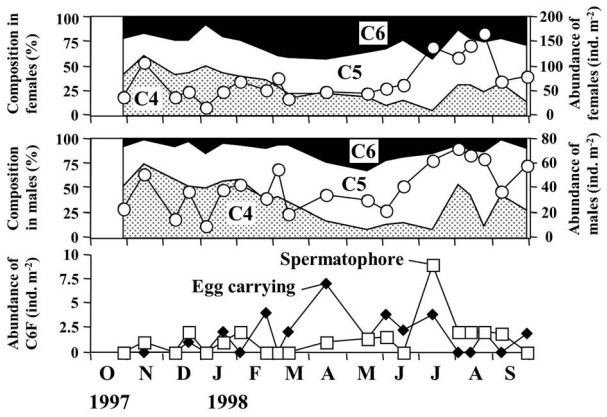

Fig. 2. *Paraeuchaeta glacialis*. Seasonal abundance and proportional changes in C4, C5 and C6 for females (upper) and males (middle). Seasonal abundance of egg carrying and spermatophore-attached adult females (C6F) (bottom).

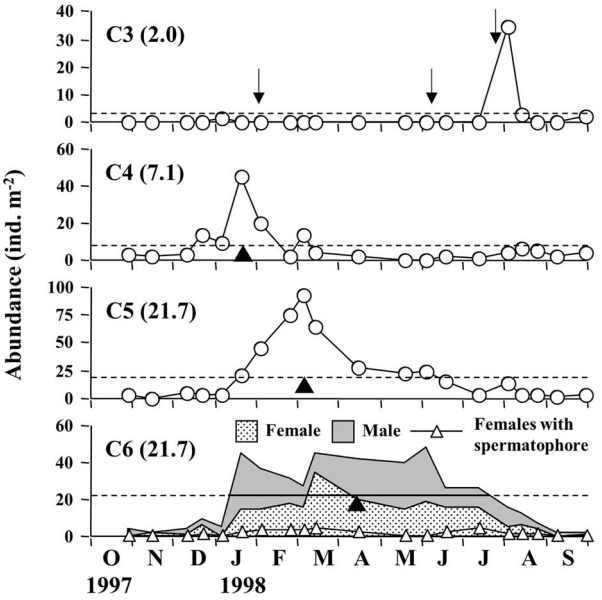

Fig. 3. *Heterorhabdus norvegicus*. Seasonal abundance of copepodite stages in the western Arctic Ocean. Values in the parentheses and horizontal broken lines indicate the annual mean abundance of each stage. Three arrows in the top panel indicate timings of water mass changes (cf. Ashjian *et al*. 2003). For the calculation of growth rate, the abundance peaks of C4 and C5 were applied. For C6, the abundant period was marked with solid horizontal lines and indicated their middle date by solid triangles. These dates marked with solid triangles were used for the growth rate calculation.

to July. The occurrence of each copepodite stage was concentrated in its abundant season, and extremely few individuals were present in the other seasons. The sex ratio could only be determined for C6. Females accounted for only 44.1 ± 11.3% of all adults, which indicated that males were dominant at the adult stage. Adult females (C6F) with spermatophores attached accounted up to 25% (11 July) of the total C6F and were abundant during December to August, which corresponded with the seasons of the highest abundance for C6M.

Vertical distribution

The $D_{50\%}$ of each copepodite stage of *P. glacialis* ranged between 74 m (C5M during the polar night) and 690 m (C6M of the polar night) (Fig. 4). Ontogenetic changes in $D_{50\%}$ were observed for the midnight sun and polar night periods ($P < 0.0001$, one-way ANOVA). Stages C1 and C6M were most abundant in the deepest layer (500–750 m), whereas C5F/M was concentrated at the shallowest depths (74–89 m). Differences in $D_{50\%}$ between the midnight sun and polar night periods were observed for C3 and C6F ($P < 0.01$, Mann–Whitney U-test). Both stages showed shallower distributions (108–156 m) during the polar night than during the midnight sun (293–468 m).

The $D_{50\%}$ of each copepodite stage of *H. norvegicus* ranged between 350 m (C3 at polar night) and 682 m (C5 at polar night) (Fig. 4). For *H. norvegicus*, no ontogenetic changes were seen for both midnight sun and polar night periods ($P = 0.327$–0.927). No temporal changes (midnight sun vs. polar night) were detected for copepodite stages.

Growth in length and weight

PG in *P. glacialis* varied considerably between females and males (Fig. 5). For females, the largest PG was observed at C5/C6 (34.0% for PL and 52.4–61.1% for weights). In contrast, for males, PG at C5/C6 was minor (6.9–22.2%), and the largest PG was observed at C4/C5, especially for weights (67.4–81.2%). In the case of *H. norvegicus*, PG was similar between females and males. In both sexes, the largest PG was observed at C5/C6, in the 28.5–30.8% and 67.9–79.3% ranges for PLs and weights, respectively.

The detailed data on the PL, weights (WW, DW, AFDW) and length–weight regressions are presented in Tables II (*P. glacialis*) and Table III (*H. norvegicus*). Weights (Y: WW, DW, AFDW, μg) and PL (X: mm) had highly significant relationships, expressed as power functions ($Y = a\ X^b$) ($r^2 = 0.961$–0.996, $P < 0.001$), with b ranging between 2.859 and 3.070 (*P. glacialis*) or 2.995–3.594 (*H. norvegicus*).

Growth rate

Based on DW, the g of *P. glacialis* was calculated for C1–C4 stages during April to November as 0.011 (Fig. 6). On the other hand, the g of *H. norvegicus* was calculated for C4–C6 during January to April as 0.035, which was much higher than that of *P. glacialis*.

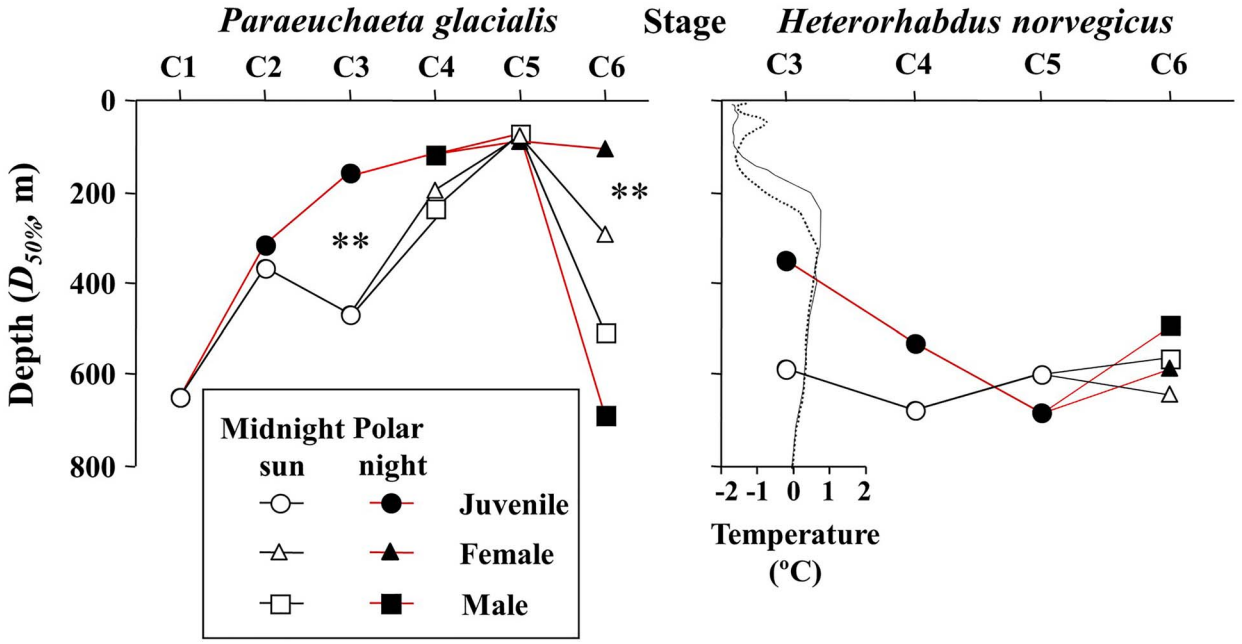

Fig. 4. *Paraeuchaeta glacialis* (left) and *Heterorhabdus norvegicus* (right). Ontogenetic changes in the mean vertical distribution centres ($D_{50\%}$, symbols) during the midnight sun (open symbols) and polar night (solid symbols). The mean temperatures during the midnight sun (solid line) and polar night (dotted line) are shown in the right panel. Asterisks indicate significant day–night differences (**$P < 0.01$; Mann–Whitney U-test).

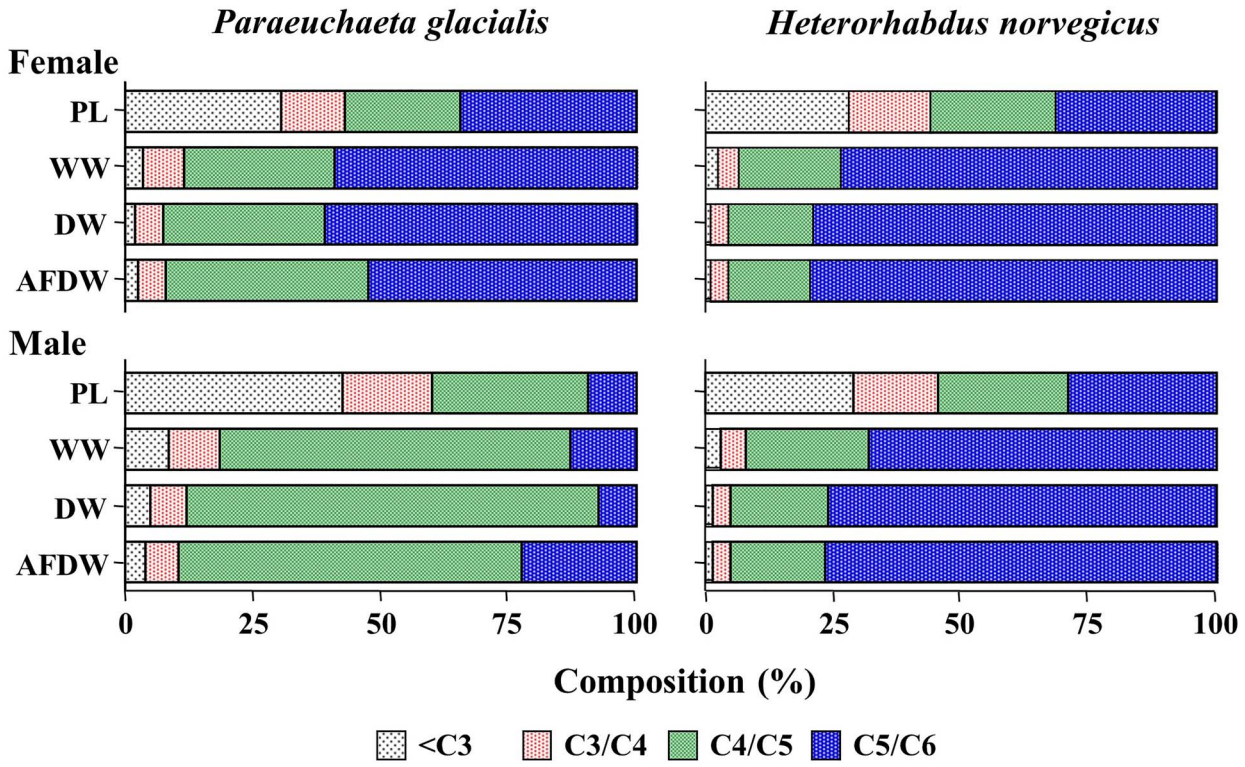

Fig. 5. *Paraeuchaeta glacialis* (left) and *Heterorhabdus norvegicus* (right). The proportion of growth (PG) in PL, WW, DW, AFDW as a percentage of the C6 values based on stage.

Table II: Paraeuchaeta glacialis. Summarized data of PL, WW, DW and AFDW

Developmental stage	PL (mm)	WW (μg)	DW (μg)	AFDW (μg)
Egg		114 ± 10	44.1 ± 2.0	41.6 ± 1.5
		(4)	(4)	(4)
Nauplius		95.1 ± 5.4	22.7 ± 1.0	21.0 ± 1.1
		(4)	(4)	(4)
C1	1.08 ± 0.04	176 ± 16	31.0 ± 1.1	28.8 ± 1.2
	(10)	(4)	(4)	(4)
C2	1.46 ± 0.09	311 ± 23	39.6 ± 2.4	33.6 ± 2.4
	(9)	(4)	(4)	(4)
C3	2.08 ± 0.10	857 ± 34	100 ± 14	80.0 ± 11.8
	(10)	(4)	(4)	(4)
C4F	2.93 ± 0.14	2990 ± 927	375 ± 73	290 ± 46
	(10)	(6)	(6)	(6)
C4M	2.94 ± 0.20	1935 ± 202	236 ± 64	231 ± 72
	(9)	(8)	(8)	(8)
C5F	4.49 ± 0.23	10 938 ± 2409	1934 ± 445	1802 ± 201
	(10)	(8)	(8)	(8)
C5M	4.43 ± 0.42	9142 ± 963	1849 ± 402	1724 ± 394
	(9)	(8)	(8)	(8)
C6F	6.80 ± 0.38	26 661 ± 2914	4965 ± 920	3784 ± 613
	(10)	(8)	(8)	(8)
C6M	4.86 ± 0.38	10 710 ± 1817	2393 ± 391	2215 ± 365
	(10)	(8)	(8)	(8)
Regression statistics for body allometry				
		WW-PL	DW-PL	AFDW-PL
	Constant (*a*)	119.4	14.96	13.27
	Power (*b*)	2.859	3.070	3.055
	r^2	0.990	0.969	0.961
	P	<0.0001	<0.0001	<0.0001

Values are mean ± standard deviation (SD). The number of replicates is in parenthesis. Body allometry was analysed using a power regression model $Y = a.X^b$, where *Y* is WW, DW or AFDW (μg) and *X* is PL (mm).

Table III: Heterorhabdus norvegicus. Summarized data of PL, WW, DW and AFDW

Developmental stage	PL (mm)	WW (μg)	DW (μg)	AFDW (μg)
C3	0.80 ± 0.03	54.0 ± 15.4	3.63 ± 0.50	3.42 ± 0.53
	(4)	(3)	(3)	(3)
C4	1.28 ± 0.05	160 ± 31	15.4 ± 1.4	13.6 ± 1.1
	(10)	(4)	(4)	(4)
C5	1.98 ± 0.07	635 ± 46	72.1 ± 8.8	63.3 ± 8.3
	(12)	(5)	(5)	(5)
C6F	2.87 ± 0.12	2375 ± 124	340.2 ± 48.9	305.2 ± 51.3
	(10)	(5)	(5)	(5)
C6M	2.77 ± 0.1	1975 ± 141	297.2 ± 33.7	269.2 ± 34.4
	(10)	(5)	(5)	(5)
Regression statistics for body allometry				
		WW-PL	DW-PL	AFDW-PL
	Constant (*a*)	90.57	7.129	6.516
	Power (*b*)	2.995	3.594	3.567
	r^2	0.993	0.996	0.995
	P	<0.001	<0.0001	<0.001

Values are mean ± standard deviation (SD). The number of replicates is in parenthesis. Body allometry was analysed using a power regression model $Y = a.X^b$, where *Y* is WW, DW or AFDW (μg) and *X* is PL (mm).

DISCUSSION

Life cycle of *P. glacialis*

Three changes in the dominant water masses in the upper layer of the SHEBA station have been reported for 1–2 February, 8–9 June and 23–24 July 1998 (Ashjian *et al.*, 2003). However, the water mass changes seem to have minimal effects on the seasonal abundance of each copepodite stage of *P. glacialis* (Fig. 1) due to the potential deeper distribution of the species. The most prominent characteristic in the population structure of *P. glacialis* was the clear seasonality in the abundance of early copepodite

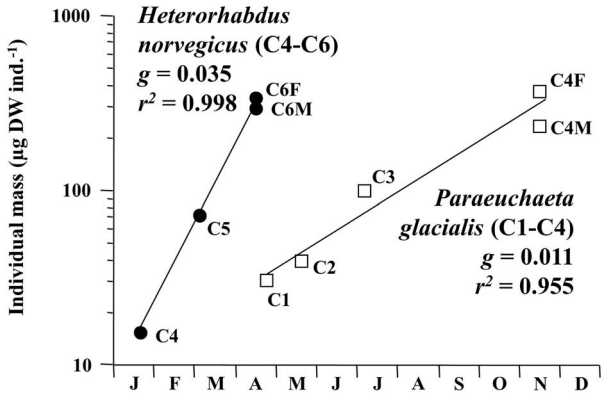

Fig. 6. Scatter plots between individual mass (μg DW ind.$^{-1}$) and season (Julian day) for C1–C4 of *Paraeuchaeta glacialis* (open squares) and C4–C6 of *Heterorhabdus norvegicus* (solid circles). The growth rates (g) were calculated for daily bases. For details, see text.

stages (Fig. 1). *Paraeuchaeta* spp. has a reproductive mode, whereby egg sacs contain a limited number of large-sized eggs, development of the naupliar stages does not require food and C1 is the first feeding stage (Campbell, 1934; Ikeda and Hirakawa, 1996).

Egg sacs of *P. glacialis* contain 46–>50 eggs (=clutch size) and the sizes of the eggs are in the 430–520-μm range in the Greenland Sea (Auel, 1999, 2004). In the Arctic Ocean, egg diameter and clutch size of *P. glacialis* have been reported to be 475–600 μm (534 ± 35 μm, mean ± 1sd) and 54–82 eggs (71.7 ± 7.6), respectively (Kosobokova *et al*., 2007). No information has been reported for egg and naupliar development in *P. glacialis*; consequently, we applied the egg hatching time (39.4 days) and naupliar development time (48.5 days) reported for the congener *Pareuchaeta elongata*, which has a similar egg diameter (500–600 μm) and was incubated under 0.5°C laboratory conditions to estimate its development (Ikeda and Hirakawa, 1996). Notably, the habitat temperature of *P. glacialis* was at −1.3–0.7°C (Fig. 4a). Based on the durations above (87.9 days = 39.4 + 48.5), the reproduction of *P. glacialis* was estimated to occur from January to March, about 90 days before the peak of C1 (April–June) (Fig. 1). Based on the year-round observation on the population structure collected by the moored sediment trap, clear seasonal recruitment of C1–C3 stages of *P. glacialis* was reported for May–July at St. NAPt in the western Arctic Ocean (Matsuno *et al*., 2014, 2015). These seasonal changes in early copepodite stages correspond well with those of this study (April–June, Fig. 1). These facts suggest the synchronized reproduction timing (January–March) was present for *P. glacialis* in the western Arctic Ocean.

Although January—March was suggested as the reproductive period, the egg-carrying females observed in the SHEBA samples were not consistent with that timing and had an abrupt peak in April (Fig. 2). This may have been due to the detachment of the egg sacs from females and loss during sampling or preservation. Such detachment from P. glacialis C6F occurred even under the stereomicroscopic observation (Yamaguchi, unpublished data). The year-round occurrence of egg-carrying females of *P. glacialis* has been reported for the western Arctic Ocean (Johnson, 1963). Notably in this study, the abundance of the egg-carrying females (between 1 and 7.5 ind. m^{-2}) was not high enough, considering the clutch sizes (46–82 eggs per sac), to maintain the peak abundance of C1 (200 ind. m^{-2}) based on the early mortality in nauplii. The other phenology demonstrated by our data was that mating occurred from July to August, confirmed by the high proportion of C6F with spermatophores attached (Fig. 2). As spermatophore was difficult to detach (Yamaguchi, unpublished data), we consider that the suggested mating period (July to August) would be a solid result.

Ontogenetic vertical migration in *Paraeuchaeta* spp. is well documented and is characterized by the deep occurrence of early copepodite stages and developmental ascent (Campbell, 1934; Morioka, 1975; Ikeda and Hirakawa, 1996; Yamaguchi and Ikeda, 2002; Yamaguchi *et al*., 2019). The deeper distribution of the early copepodite stages may reduce mortality (Yamaguchi and Ikeda, 2002; Yamaguchi *et al*., 2019). The developmental ascent from 690 m (C1) to 74 m (C5) was demonstrated here for *P. glacialis* (Fig. 4). Particularly, the vertical distribution within the stage was shallower at polar night than at midnight sun, excluding in the case of C6M (Fig. 4). Since visual predation impact is expected to be high during the midnight sun, the deeper occurrence at the period may be related to predation avoidance. Arctic cod have been reported to be key predators of *P. glacialis* (Majewski *et al*., 2016). Notably, the shallowest distributed stage (C5) was the only stage that revealed no differences in vertical distribution between midnight sun and polar night (Fig. 4). It may be attributed to the C5 stage being the active predator facilitating massive growth, especially in weight (Fig. 5). For greater growth, the C5 stage may stay at the shallower depths (74 m), where food is abundant both at midnight sun and at polar night.

Life cycle of *H. norvegicus*

Because of the species' long generation length, seasonality was relatively obscured at the mid- to late-copepodite stages of *P. glacialis*. By contrast, clear seasonality was evident for all observed copepodite stages (C3–C6) of *H. norvegicus*, and the abundance of the other seasons was extremely low for all the stages (Fig. 3), suggesting that

H. norvegicus produced one cohort per year with a 1-year generation length.

For *H. norvegicus*, the sexes could only be distinguished at the adult stage. The sex ratio was nearly 1:1 or skewed towards males (Table I). The dominance of males in *H. norvegicus* adults has also been reported for the western Arctic Ocean based on year-round sediment trap observations (annual mean C6F: total C6 = 39.8%) (Tokuhiro *et al*., 2019). For a congener species in the western subarctic Pacific (*Heterorhabdus tanneri*), the dominance of males (annual mean C6F: total C6 = 45.3%) has also been reported following year-round observation (Yamaguchi and Ikeda, 2000b). A skewed sex ratio towards males, which has been documented for *Heterorhabdus* species from three regions, is a unique characteristic of the genus. In general, various mesopelagic copepods with a body size similar to that of *Heterorhabdus* spp. (e.g. Euchaetidae, Aetideidae, Scolecitrichidae) have degeneration of feeding appendages and cease feeding at C6M, which may induce short longevity of C6M and skewed sex ratio to C6F in adults (Yamaguchi and Ikeda, 2000a, 2002; Yamaguchi *et al*., 2020). However, *Heterorhabdus* have functional feeding appendages even at C6M (Brodsky, 1950) and have longer longevity, which likely contributes to the skewed sex ratio towards males. Such longevity enhances the chances of mating and fertilization.

The specialized raptorial feeding modes of *Heterorhabdus* species are quite distinct from the sympatric *Paraeuchaeta* species (Lewis, 2014). According to Nishida and Ohtsuka (1996), a specialized feeding mechanism, wherein venom or anaesthetic is injected from the labral-gland pores into the tubular lumen of the mandibular ventral-most tooth, has been proposed. The labrum–paragnath complex of *Heterorhabdus* spp. is beak-like and has a much larger mouth than other similar sized copepod species (Lewis, 2014). The much faster growth rate ($g = 0.035$) of *H. norvegicus* than that of the sympatric *P. glacialis* ($g = 0.011$) may be related to the specialized feeding modes of *Heterorhabdus* species (Fig. 6).

The specialized ecology of *Heterorhabdus* spp. is also apparent in their reproduction. *H. norvegicus* shed 93 and 95 eggs freely, with a diameter of 150–157 μm (Kosobokova *et al*., 2007). Thus, their reproduction would be characterized by a large number of small-sized eggs. As most of the deep-sea copepods produce a small number of large-sized eggs (cf. Marshall, 1979; Herring, 2002), the reproduction mode of *H. norvegicus* is anomalous for a mesopelagic species.

From sediment traps moored at St. NAPt in the western Arctic Ocean, *H. norvegicus* C1 and C2 occurred in June–July, C6M outnumbered C6F throughout the year and reproduction occurred in April–May (Matsuno *et al*., 2014). The seasonal abundance of early copepodite stages (C1–C2) was consistent with that of later stages observed in this study (C3 occurred in August). The dominance of C6M in the adult population was also consistent with this study's observations. In a later study, using 2 years of sediment trap data, the life cycle of *H. norvegicus* was revised to show that C1 was most abundant in April–May, C5 and C6M were dominant in November–February and August–October respectively, and reproduction occurred in February–March (Matsuno *et al*., 2015). The observed *H. norvegicus* reproduction during a limited period may be reflected in the sharp C3 peak in August in this study (Fig. 3). Together, the findings suggest that the life cycle of *H. norvegicus* has a 1-year generation length with the main period of reproduction being from February to March. The slight differences in abundant seasons (1 or 2 months) of each copepodite stage between the studies may be caused by the regional differences in phenology (ice cover, peak of primary productivity, zooplankton abundance and biomass) which varied greatly within the Arctic Ocean (Søreide *et al*., 2010; Bélanger *et al*., 2013; Ji *et al*., 2013; Steele and Dickinson, 2016).

CONCLUSIONS

Based on the time-series of year-round, vertical stratified net tows of zooplankton samples conducted at the SHEBA ice-station in the Arctic Ocean, ecological characteristics (population structure, vertical distribution and length and weight growth) were compared for the two dominant sympatric mesopelagic carnivorous copepods (*P. glacialis* and *H. norvegicus*). The reproductive timings of the two species were similar, occurring from January to March. Vertical distribution and PG between stages varied between the species. For *P. glacialis*, early copepodite stages and C6M occurred in the deepest layers, apparently to reduce mortality due to predation by visual predators. In contrast, for *H. norvegicus*, all developmental stages occurred in the same mesopelagic layers, and they exhibited faster growth that seemed to allow them to have shorter 1-year generation lengths. Although their habitat (mesopelagic) is characterized by limited food resources, *H. norvegicus* had a faster growth rate and shorter generation length. The specialized feeding mode (armored venom injection teeth and large-beak labrum) of *H. norvegicus* could be essential for achieving such rapid growth rates in the mesopelagic zone.

ACKNOWLEDGEMENTS

We thank the crew members of the CCGS *Des Groseilliers* and the SHEBA project members, especially Harold "Buster" Welch, for

assistance in collecting samples and CTD data. The constructive comments by the anonymous reviewers were very helpful and greatly improved the text.

FUNDING

The collection of the samples was supported in part by grants #OCE9707184 to C.J. Ashjian and #OCE9707182 to R.G. Campbell from the US National Science Foundation. Y. Abe assisted figure illustration. This work was partially supported by the Arctic Challenge for Sustainability II (ArCS II), Program Grant Number JPMXD1420318865. This research was also supported by the Environment Research and Technology Development Fund (JPMEERF20214002) of the Environmental Restoration and Conservation Agency of Japan. In addition, this work was partly supported by a Grant-in-Aid for Challenging Research (Pioneering) JP20K20573, and Scientific Research JP22H00374 (A), JP20H03054 (B), JP19H03037 (B), JP21H02263 (B) and JP17H01483 (A) from the Japanese Society for the Promotion of Science (JSPS).

REFERENCES

Ashjian, C. J., Campbell, R. G., Welch, H. E., Butler, M. and Van Keuren, D. (2003) Annual cycle in abundance, distribution, and size in relation to hydrography of important copepod species in the western Arctic Ocean. *Deep Sea Res. I*, **50**, 1235–1261.

Auel, H. (1999) The ecology of Arctic deep-sea copepods (Euchaetidae and Aetideidae). Aspects of their distribution, trophodynamics and effect on the carbon flux. *Ber. Polarforsch.*, **319**, 1–97.

Auel, H. (2004) Egg size and reproductive adaptations among Arctic deep-sea copepods (Calanoida, *Paraeuchaeta*). *Helgol. Mar. Res.*, **58**, 147–153.

Bélanger, S., Babin, M. and Tremblay, J.-É. (2013) Increasing cloudiness in Arctic damps the increase in phytoplankton primary production due to sea ice receding. *Biogeosciences*, **10**, 4087–4101.

Brodsky, K. A. (1950, 1967) Copepoda Calanoida of the far-eastern seas of the USSR and Arctic Seas. Akad. Nauk SSSR Zool. *Inst. Opred. Faune SSSR*, **35**, 1–442 (in Russian).

Campbell, M. H. (1934) The life history and post embryonic development of the copepods, *Calanus tonsus* Brady and *Euchaeta japonica* Marukawa. *J. Biol. Bd. Can.*, **1**, 1–65.

Conover, R. J. (1988) Comparative life histories in the genera *Calanus* and *Neocalanus* in high latitudes of the northern hemisphere. *Hydrobiologica*, **167/**168, 127–142.

Dvoretsky, V. G. and Dvoretsky, A. G. (2015) Summer population structure of the copepods *Paraeuchaeta* spp. in the Kara Sea. *J. Sea Res.*, **96**, 18–22.

Herring, P. (2002) *The Biology of the Deep Ocean*, Oxford University Press, Oxford, p. 314.

Hirst, A. G., Roff, J. C. and Lampitt, R. S. (2003) A synthesis of growth rates in marine epipelagic invertebrate zooplankton. *Adv. Mar. Biol.*, **44**, 1–142.

Ikeda, T. and Hirakawa, K. (1996) Early development and estimated life cycle of the mesopelagic copepod *Pareuchaeta elongata* in the southern Japan Sea. *Mar. Biol.*, **126**, 261–270.

Ji, R., Jin, M. and Varpe, Ø. (2013) Sea ice phenology and timing of primary production pulses in the Arctic Ocean. *Glob. Change Biol.*, **19**, 734–741.

Johnson, M. W. (1963) Zooplankton collections from the high polar basin with special reference to the Copepoda. *Limnol. Oceanogr.*, **8**, 89–102.

Kosobokova, K. N. (1982) Composition and distribution of the biomass of zooplankton in the central Arctic Basin. *Oceanology*, **22**, 744–750.

Kosobokova, K. and Hirche, H.-J. (2000) Zooplankton distribution across the Lomonosov Ridge, Arctic Ocean: species inventory, biomass and vertical structure. *Deep Sea Res. I*, **47**, 2029–2060.

Kosobokova, K. N. and Hopcroft, R. R. (2010) Diversity and vertical distribution of mesozooplankton in the Arctic's Canada Basin. *Deep Sea Res. II*, **57**, 96–110.

Kosobokova, K. N., Hirche, H.-J. and Hopcroft, R. R. (2007) Reproductive biology of deep-water calanoid copepods from the Arctic Ocean. *Mar. Biol.*, **151**, 919–934.

Kosobokova, K. N., Hopcroft, R. R. and Hirche, H.-J. (2011) Patterns of zooplankton diversity through the depths of the Arctic's central basins. *Mar. Biodivers.*, **41**, 29–50.

Lewis, A. (2014) A comparison of the labrum-paragnath complex in five species of calanoid copepods. *Crustaceana*, **87**, 1200–1224.

Majewski, A. R., Walkusz, W., Lynn, B. R., Atchison, S., Eert, J. and Reist, J. D. (2016) Distribution and diet of demersal Arctic cod, *Boreogadus saida*, in relation to habitat characteristics in Canadian Beaufort Sea. *Polar Biol.*, **39**, 1087–1098.

Marshall, N. B. (1979) *Developments in Deep-Sea Biology*, Blandford Press, Poole, Dorset, p. 566.

Matsuno, K., Yamaguchi, A., Fujiwara, A., Onodera, J., Watanabe, E., Imai, I., Chiba, S., Harada, N. *et al.* (2014) Seasonal changes in mesozooplankton swimmers collected by sediment trap moored at a single station on the Northwind Abyssal Plain in the western Arctic Ocean. *J. Plankton Res.*, **36**, 490–502.

Matsuno, K., Yamaguchi, A., Fujiwara, A., Onodera, J., Watanabe, E., Harada, N. and Kikuchi, T. (2015) Seasonal changes in the population structure of dominant planktonic copepods collected using a sediment trap moored in the western Arctic Ocean. *J. Nat. Hist.*, **49**, 2711–2726.

Morioka, Y. (1975) A preliminary report on the distribution and life history of a copepod *Pareuchaeta elongata* in the vicinity of Sado Island, the Japan Sea. *Bull. Japan Sea Reg. Fish. Res. Lab.*, **26**, 41–56.

Nishida, S. and Ohtsuka, S. (1996) Specialized feeding mechanism in the pelagic copepod genus *Heterorhabdus* (Calanoida: Heterorhabdidae), with special reference to the mandibular tooth and labral glands. *Mar. Biol.*, **126**, 619–632.

Smoot, C. A. and Hopcroft, R. R. (2017) Depth-stratified community structure of Beaufort Sea slope zooplankton and its relations to water masses. *J. Plankton Res.*, **39**, 79–91.

Søreide, J., Leu, E., Berge, J., Graeve, M. and Falk-Petersen, S. (2010) Timing of blooms, algal food quality and *Calanus glacialis* reproduction and growth in a changing Arctic. *Glob. Chang. Biol.*, **16**, 3154–3163.

Steele, M. and Dickinson, S. (2016) The phenology of Arctic Ocean surface warming, *J. Geophys. Res.*, **121**(C), 6847–6861.

Tokuhiro, K., Abe, Y., Matsuno, K., Onodera, J., Fujiwara, A., Harada, N., Hirawake, T. and Yamaguchi, A. (2019) Seasonal phenology of four dominant copepods in the Pacific sector of the Arctic Ocean: insights from statistical analyses of sediment trap data. *Polar Sci.*, **19**, 94–111.

Yamaguchi, A. and Ikeda, T. (2000a) Vertical distribution, life cycle and developmental characteristics of mesopelagic calanoid copepod *Gaidius variabilis* (Aetideidae) in the Oyashio region, western North Pacific Ocean. *Mar. Biol.*, **137**, 99–109.

Yamaguchi, A. and Ikeda, T. (2000b) Vertical distribution, life cycle, and body allometry of two oceanic calanoid copepods (*Pleuromamma scutullata* and *Heterorhabdus tanneri*) in the Oyashio region, western North Pacific Ocean. *J. Plankton Res.*, **22**, 29–46.

Yamaguchi, A. and Ikeda, T. (2002) Reproductive and developmental characteristics of three mesopelagic *Paraeuchaeta* species (Copepoda: Calanoida) in the Oyashio region, western subarctic Pacific Ocean. *Bull. Fish. Sci. Hokkaido Univ.*, **53**, 11–21.

Yamaguchi, A., Ashjian, C. J., Campbell, R. G. and Abe, Y. (2019) Ontogenetic vertical migration of the mesopelagic carnivorous copepod *Paraeuchaeta* spp. is related to their increase in body mass. *J. Plankton Res.*, **41**, 791–797.

Yamaguchi, A., Ashjian, C. J., Campbell, R. G. and Abe, Y. (2020) Vertical distribution, population structure and developmental characteristics of the less studied but globally distributed mesopelagic copepod *Scaphocalanus magnus* in the western Arctic Ocean. *J. Plankton Res.*, **42**, 368–377.